Computation of Strongly Swirling Axisymmetric Free Jets

M.A. Leschziner*
University of Manchester Institute of Technology, Manchester, Great Britain
and
W. Rodi†
University of Karlsruhe, Karlsruhe, Federal Republic of Germany

Finite difference computations have been performed of strongly swirling circular free jets operating at swirl numbers of 1.18 and 1.3. These values are sufficiently high for recirculation to occur near the jet nozzle. The study focuses on the response of the computed flowfield to the introduction of swirl-related modifications into the k-ϵ model of turbulence, and to changes in the boundary conditions for the dissipation rate ϵ and the radial velocity V at the computational jet inlet plane. It is shown that the inlet conditions for V and ϵ, usually considered of subordinate importance, play as crucial a role in achieving predictive accuracy as turbulence-modeling details. In particular, it is found that, with a realistic V distribution prescribed at the jet-inlet plane, satisfactory predictions can be obtained without any swirl-specific modifications to the k-ϵ model. While it is not argued that such modifications are generally redundant and inappropriate, it is suggested that any attempt to identify and rectify turbulence-model defects is bound to be frustrated unless comprehensive experimental data for all flow properties at the jet exit become available.

Nomenclature

A_W, A_E, A_S, A_N, A_P = finite difference coefficients, Eq. (12)
c_1, c_2, c_μ = empirical turbulence-model coefficients, Eqs. (5) and (7)
d = jet diameter
f_1, f_2 = swirl-related correction terms in turbulence model, Eqs. (8) and (9)
G = rate of generation of k, Eq. (6)
k = turbulence energy
L = turbulence length scale, Eq. (10)
P = static pressure
R_i, R_f = gradient and flux Richardson numbers, respectively, Eqs. (8) and (9)
r = radial coordinate
$r_{1/2}$ = jet half-width
S = swirl number,

$$\equiv \int_o^\infty r^2 UW \mathrm{d}r / \mathrm{d} \Big/ 2 \int_o^\infty (U^2 - W^2/2) r \mathrm{d}r$$

S_Φ, S_V = source terms for scalar Φ and velocity V, Eqs. (12) and (14)
U, V, W = axial, radial, and tangential velocity components, respectively
$U_m, U_{m,0}$ = maximum U velocity at any axial location and at jet exit, respectively
U_ℓ = centerline U velocity
$\overline{u^2}, \overline{v^2}, \overline{w^2}, \overline{uv}$ = Reynolds stresses
$W_m, W_{m,0}$ = maximum tangential velocity at any axial location and at jet exit, respectively
x = axial coordinate
α = numerical coefficient, Eq. (13)
$\delta_{0.1}$ = jet thickness (determined by 10% velocity locations)
ϵ = turbulence-energy dissipation
ν_t, ν = kinematic eddy and fluid viscosity, respectively
ρ = fluid density
$\sigma_k, \sigma_\epsilon$ = Prandtl/Schmidt numbers for k and ϵ, respectively, Eqs. (6) and (7)
Φ = any conserved scalar property
ψ = streamfunction

Received July 5, 1983; revisions received Dec. 2, 1983.

*Lecturer, Department of Mechanical Engineering.
†Professor, Institut für Hydromechanik. Member AIAA.

I. Introduction

SWIRL imparted to circular jets is an important, often essential operational feature in a number of engineering applications. Prominent among these are flames in gas turbine and furnace combustors in which swirl strongly contributes to efficiency of combustion by enhancing mixing, and to flame stability through recirculation. Substantial efforts, both experimental and computational, have thus been made over the past decade[1,2] to study and analyze the complex hydrodynamic and heat-transfer processes in turbulent swirling jets and flames. Such studies, particularly at high-swirl intensities at which regions of recirculation arise, have been fraught with difficulties even under nonreacting isothermal conditions. Measurement techniques, involving physical probes such as hot wires and five-hole tubes, pose problems due to the high sensitivity of swirling flows to internal obstructions.[3,4] Moreover, the above probes do not, in general, allow resolution of flow direction. Laser-Doppler anemometry, on the other hand, suffers from seeding particle depletion and inhomogeneities within the flow because of strong centrifugal effects.[5]

Computational studies are subject to even more serious uncertainties. Combustion modeling apart, major difficulties arise in relation to turbulence modeling,[6-8] discretization errors associated with upwind differencing of the convection terms in the equations,[9] and a lack of knowledge about the boundary conditions. In general, errors arising from the sources just mentioned occur simultaneously and cannot be separated. Only at low-swirl intensities (swirl numbers $S \leq 0.5$), when recirculation is absent and the governing equations are parabolic in character, can errors due to turbulence-model defects be identified unambiguously, for then discretization errors are minor, and accurate initial conditions can readily be extracted from carefully controlled ex-

periments. Such computations have shown[8,10] that isotropic-eddy-viscosity closures, whether of the algebraic type or involving differential equations for the velocity and length scales of turbulence, fail to mimic the effects of swirl on the rate of spread, velocity decay, and anisotropy of shear stresses unless swirl-related ad-hoc modifications are introduced. A number of such corrections, all intended to yield no more than the correct mean-flow behavior, have been proposed and used.[7,8,10,11] All involve either gradient or flux Richardson number dependent terms modifying either the eddy viscosity directly or the turbulent length scale, so as to account phenomenologically for the effect of streamline curvature on turbulent transport.

Recirculation due to strong swirl must be expected to aggravate the turbulence-model defects just mentioned. Yet, the picture emerging here from a review of previous work is less clear. A few computational studies do, indeed, support the conclusion that the standard model with isotropic eddy viscosity and no extra swirl-related terms yields poor predictions also for strongly swirling jets.[12,13] Agreement with experimental data is here again achieved either through Richardson number type corrections or, in a very recent study,[13] with the aid of a particular algebraic Reynolds stress closure. (Such a type of closure, albeit involving a different pressure-strain model, has not proved itself in weakly swirling jets.[6]) Yet, there exist also a number of studies[14-17] which demonstrate satisfactory agreement without swirl-related corrections.

The question thus arises as to what extent the turbulence-model performance has been obscured by errors arising from other sources, in particular ill-prescribed boundary conditions. It is this question to which the present paper addresses itself.

Computations with the standard k-ϵ model and with two versions involving swirl modifications are presented for strongly swirling circular free jets subject to various conditions at the upstream boundary. The flowfield of such jets, in particular the recirculation region, is especially sensitive to swirl and, consequently, the representation of its effects within a turbulence model. A further positive feature of circular jets in the context of this study is the large aspect ratio of the recirculation bubble, which minimizes numerical errors, resulting from flow-to-grid skewness when convection is approximated by an upwind scheme. The cases simulated are those investigated experimentally by Curtet and Darrigol[18] and Hösel,[5] and the paper discusses the influence of variations in the upstream boundary conditions on the results obtained with the turbulence-model versions used.

II. Mathematical Model

A. Mean-Flow Equations

The flowfield of axisymmetric swirling jets, as sketched in Fig. 1, is governed by the equations for the axial, radial, and tangential momentum components and the continuity equations. On the assumption of an isotropic eddy viscosity in the stress-strain relationship, these equations become:

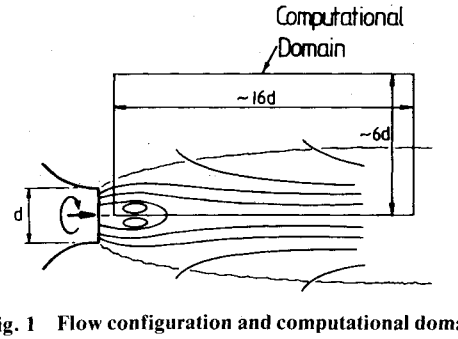

Fig. 1 Flow configuration and computational domain.

U momentum

$$\frac{\partial U^2}{\partial x}+\frac{1}{r}\frac{\partial rUV}{\partial r}=-\frac{1}{\rho}\frac{\partial P}{\partial x}+\frac{\partial}{\partial x}\left(2\nu_t\frac{\partial U}{\partial x}\right)+\frac{1}{r}\frac{\partial}{\partial r}\left[r\nu_t\left(\frac{\partial U}{\partial r}+\frac{\partial V}{\partial x}\right)\right] \tag{1}$$

V momentum

$$\frac{\partial UV}{\partial x}+\frac{1}{r}\frac{\partial rV^2}{\partial r}=-\frac{1}{\rho}\frac{\partial P}{\partial r}+\frac{W^2}{r}+\frac{\partial}{\partial x}\left[\nu_t\left(\frac{\partial V}{\partial x}+\frac{\partial U}{\partial r}\right)\right]+\frac{1}{r}\frac{\partial}{\partial r}\left(2r\nu_t\frac{\partial V}{\partial r}\right)-2\nu_t\frac{V}{r^2} \tag{2}$$

Wr momentum

$$\frac{1}{r}\frac{\partial rUW}{\partial x}+\frac{1}{r}\frac{\partial r^2VW}{\partial r}=\frac{\partial}{\partial x}\left(\nu_t\frac{\partial rW}{\partial x}\right)+\frac{1}{r}\frac{\partial}{\partial r}\left(r\nu_t\frac{\partial rW}{\partial r}\right)-\frac{2}{r}\frac{\partial}{\partial r}(\nu_t rW) \tag{3}$$

Continuity

$$\frac{\partial U}{\partial x}+\frac{1}{r}\frac{\partial rV}{\partial r}=0 \tag{4}$$

B. Turbulence Models

Effects of turbulence, which enter the preceding equations through the eddy viscosity ν_t, are represented by the so-called standard k-ϵ model, as described by Launder and Spalding,[19] and two variants of this. The standard version relates the eddy viscosity to the turbulent kinetic energy k and the dissipation rate ϵ via

$$\nu_t=c_\mu k^2/\epsilon \tag{5}$$

and determines the distribution of k and ϵ from the following transport equations.

$$\frac{\partial Uk}{\partial x}+\frac{1}{r}\frac{\partial rVk}{\partial r}=\frac{\partial}{\partial x}\left(\frac{\nu_t}{\sigma_k}\frac{\partial k}{\partial x}\right)+\frac{1}{r}\frac{\partial}{\partial r}\left(\frac{r\nu_t}{\sigma_k}\frac{\partial k}{\partial r}\right)+G-\epsilon \tag{6}$$

$$\frac{\partial U\epsilon}{\partial x}+\frac{1}{r}\frac{\partial rV\epsilon}{\partial r}=\frac{\partial}{\partial x}\left(\frac{\nu_t}{\sigma_\epsilon}\frac{\partial \epsilon}{\partial x}\right)+\frac{1}{r}\frac{\partial}{\partial r}\left(\frac{r\nu_t}{\sigma_\epsilon}\frac{\partial \epsilon}{\partial r}\right)+\frac{\epsilon}{k}(c_1G-c_2\epsilon) \tag{7}$$

where

$$G\equiv\nu_t\left\{2\left[\left(\frac{\partial U}{\partial x}\right)^2+\left(\frac{\partial V}{\partial r}\right)^2+\left(\frac{V}{r}\right)^2\right]+\left(\frac{\partial U}{\partial r}+\frac{\partial V}{\partial x}\right)^2+\left(\frac{\partial W}{\partial x}\right)^2+\left[r\frac{\partial}{\partial r}\left(\frac{W}{r}\right)\right]^2\right\}$$

is the production of k by the mean-velocity gradients, and $c_\mu=0.09$, $\sigma_k=1$, $\sigma_\epsilon=1.22$, $c_1=1.44$, $c_2=1.92$ are empirical constants.

The two variants of the given model involve corrections introduced to the length-scale determining ϵ-equation (7), which are meant to account for the effect of streamline curvature due to swirl. The first correction is that of Launder et al.[11] and can be expressed as a function f_1 multiplying c_2 in

Eq. (7), viz.

$$f_1 = 1 - 0.2\,Ri \tag{8}$$

where Ri is a gradient Richardson number defined by

$$Ri \equiv \frac{k^2}{\epsilon^2}\frac{W}{r^2}\frac{\partial rW}{\partial r}$$

The second correction suggested and used by Rodi[8] for weakly swirling jets can be expressed as a function f_2 multiplying c_1 in Eq. (7), viz.

$$f_2 = 1 + 0.9R_f \tag{9}$$

where R_f is a flux Richardson number defined by

$$R_f \equiv \left(2\nu_t W\frac{\partial W/r}{\partial r}\right)\Big/G$$

Both corrections are based on the hypothesis that the destabilizing (or turbulence-amplifying) effect of swirl is primarily due to or can be modeled through an increase in the length scale of the energetic turbulent eddies. Yet, the detailed interpretation of the mechanism by which the increase occurs is different. The LPS correction Eq. (8) is essentially a result of qualitative considerations on the stabilizing or destabilizing influence of a radially varying body-force field $\rho W^2/r$ on the lateral turbulent fluctuations.[20] Correction Eq. (9), in contrast, relates length-scale changes to the extra production of radial fluctuations due to the centripetal body-force term. The difference is by no means cosmetic, for correction Eq. (8) predicts a turbulence-damping effect over large regions of a swirling jet in which $\partial Wr/\partial r$ is positive, while correction Eq. (9) tends to amplify turbulence regardless of the sign of $\partial Wr/\partial r$.

C. Boundary Conditions

Fluid recirculation demands that an elliptic procedure be used for solution. This requires the prescription of conditions on all boundaries of the solution domain shown in Fig. 1. Four types of boundaries need consideration, namely, inlet, outlet, axis of symmetry, and entrainment boundary. Conditions along the inlet plane demand particularly careful attention because these exert a crucial effect on the predicted flowfield, as will be shown subsequently. In both jets simulated here, measurements were performed at axial planes close to but not coincident with the jet exit; it is for this reason that the computational inlet planes lie at $x/d=0.75$ and 1.0 in Hösel's and Curtet and Darrigol's jets, respectively. While distributions of axial and swirl velocities at two planes were directly available, data for V, k, and ϵ were not.

In Hösel's case, where the computational inlet was placed at $x/d=0.75$, two alternative V profiles were prescribed; the first being, simply, $V=0$ (a frequent assumption) and the second extracted from the streamfunction-contour plot $\psi(x,r)$ shown in Fig. 2 and obtained by integrating $\partial\psi/\partial r=\rho rU(r)$ at various axial locations. The turbulence energy k could be obtained with some confidence from measurements for u^2 and w^2 with values for v^2 assumed to be $0.5(u^2+w^2)$. A high degree of uncertainty arises, unfortunately, in relation to ϵ; this could have been extracted from k and uv had the latter been measured. In the absence of such data at $x/d=0.75$, a reference distribution was determined from

$$\epsilon = k^{3/2}/L \quad \text{with} \quad L = 0.075\delta_{0.1}/c_\mu{}^{3/4} \tag{10}$$

where $\delta_{0.1}$ is the jet width defined by the locations at which $U=0.1U_{\max}$. The preceding is essentially a mixing-length prescription. Eddy viscosities thus obtained were of the order of 700μ over a major portion of the shear layer. This figure is, of course, somewhat speculative but supported to an extent by a similar level extracted from Curtet and Darrigol's data for U and uv at $x/d=1$ through the relationship

$$\epsilon = c_\mu\frac{k^2}{\rho\overline{uv}}\frac{\partial U}{\partial r} \tag{11}$$

It must be stated, however, that no data for k were provided by Curtet and Darrigol. Thus, the just stated level of ϵ rests on the assumption that the dimensionless distribution $k/U^2{}_{\max}=f(r/r_{1/2})$ of Curtet and Darrigol at $x/d=1$ is identical to that of Hösel at $x/d=0.75$, from which the inlet k distribution for Curtet and Darrigol's jet was extracted. There is clearly, yet again, an element of uncertainty attached to the preceding treatment; this is, however, supported by the close similarity of the axial and swirl velocity profiles of the two jets at their respective inlet planes. At the axis of symmetry, the radial velocity V and the radial gradients of all remaining flow properties were set to zero. The preceding is clearly invalid for the swirl velocity W.

However, it is not W but (Wr) which is the property governed by Eq. (3): a zero gradient assumption for the latter is appropriate. Across the exit plane, approximately 16 diameters from the jet, the axial pressure gradient $\partial P/\partial x$ was assumed to be zero. At this location swirl and its gradient are so weak that deviations from this assumption do not exert more than a marginal influence in the immediate vicinity of the exit plane. The exit U velocity was computed from the usual momentum balance, as performed for the internal region. Since this velocity is positive and its streamwise gradient is low, any downstream-to-upstream link is negligibly weak and no boundary conditions for velocity are required. Along the entrainment boundary, which was placed sufficiently far away from the axis of symmetry, the static pressure was assumed constant (conveniently zero). The axial velocity U was assumed zero while k and ϵ were assigned arbitrarily low values yielding an eddy viscosity $\nu_t = 10\nu$. With U and P known, the entrainment velocity V was computed as an integral part of the solution process by solving Eq. (2) with the assumptions $P=0$, $U=0$, and $Vr=$ const just outside the domain of solution.

D. Solution Procedure

Solutions were obtained with the computer code TEACH of Gosman and Pun.[21] The procedure is based on the finite volume approach with diffusion approximated by central differences and convection modeled through a hybrid central/upwind-difference scheme. For any dependent variable Φ, the partial differential equation is represented by a coupled set of algebraic equations of the form

$$A_P\Phi_P = \Sigma A_i\Phi_i + S_{\Phi,P} \qquad i=\text{N,S,E,W} \tag{12}$$

where P,N,S,E,W denote mesh nodes and S_Φ is the source term in the equation for Φ.

The computational mesh used for all calculations consisted of 30×30 nonuniformly distributed nodes with a high grid-line concentration within and in the vicinity of the recirculation region. The grid extended to an axial distance of $x/d\cong16$ and a radial distance of $r/d\cong6$. Grid expansion factors did not exceed 1.2. No credible grid-dependence tests could be carried out with finer meshes because of computer-resource limitations. However, test computations performed with a mesh similar to that just mentioned for Morse's[2] weakly swirling jet at $S=0.36$ compared very favorably with corresponding computations of Rodi[8] carried out with the boundary-layer code GENMIX. While the occurrence of recirculation at the higher swirl numbers examined here is likely to demand an increase in mesh density for equal ac-

curacy, this increase is unlikely to be substantial. This is because the recirculation region is small and highly elongated, in which case errors arising from flow-to-grid skewness are likely to be minor.

Because of the strong swirl and the resulting strong coupling between Eqs. (3) and (4), stability was difficult to maintain and convergence was relatively slow. Measures needed to achieve convergence included 1) a gradual introduction of swirl; 2) fairly strong underrelaxation in the solution of the equations; and 3) a partial coupling of the body-force term W^2/r, which is the principal source of radial momentum in Eq. (2), to the field of the radial velocity V as suggested by Gosman et al.[22]:

$$\frac{W^2}{r} \Rightarrow \frac{W^2}{r}\left[1+\frac{\alpha}{W}\left(V^{(m-1)}-V^{(m)}\right)\right] \tag{13}$$

where $\alpha=2$ was found to be adequate, and (m) denotes the current iteration level. Replacement (13) (which becomes an identity when the solution has converged) allows Eq. (12), with $\Phi=V$, to be written as

$$\left(A_P+\frac{\alpha W}{r}\Delta r\Delta x\right)V_P^{(m)} = \sum_{i=\mathrm{N,S,W,E}} A_i V_i^m + \left(1+\frac{\alpha}{W}V^{(m-1)}\right)\frac{W^2}{r}\Delta r\Delta x + S'_{V,P} \tag{14}$$

It is principally the augmentation of A_P in Eq. (14) which is responsible for the increased stability. With the measures just given, the number of iterations required to reduce momentum and mass sources to below 0.5% of respective jet-inlet values ranged from 400 for the standard k-ϵ model to 800 for the version incorporating Rodi's modification.[9] Computing (CPU) times were of the order of 3 s per iteration on a UNIVAC 1108 computer.

III. Discussion of Results

A major objective of the computations performed is to examine the sensitivity of mean-flow parameters such as half-width, centerline velocity, and maximum axial and swirl velocity to changes in inlet conditions, and to contrast this with the response to variations in the turbulence model. Specifically, the effects of V and ϵ, whose distributions are frequently assumed and accepted without argument, are considered. The intention is to determine whether boundary-condition related errors could mask effects of turbulence-model modifications, thus putting in doubt, if not invalidating, previous conclusions on the adequacy of the models. An experimentally observed feature of considerable bearing on the present discussion is the very different near-field spreading behavior of the two jets examined, as seen from Fig. 3. This difference is puzzling for in both cases swirl is generated through tangential slot injection, the swirl numbers are of similar magnitude, and the inlet profiles, if nondimensionalized as $U/U_m=f(r/r_{1/2})$, $W/W_m=g(r/r_{1/2})$, are similar.

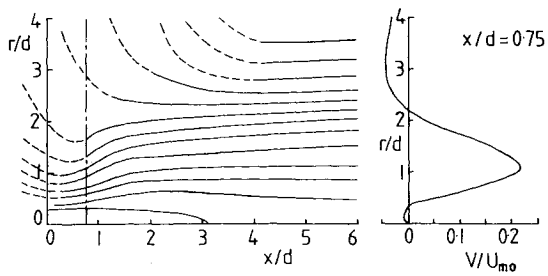

Fig. 2 Streamlines and V-profile at $x/d=0.75$ determined from Hösel's[5] U-velocity measurements.

There appear to be two possible sources for the stated feature. First, substantially different turbulence structures and/or levels prevailed, leading to different rates of entrainment close to the exit. Second, inertial effects due to the imbalance between the radial pressure gradient and centrifugal acceleration differed substantially, resulting in very different radial velocity levels at the inlet.

The former process, if not captured by the turbulence model itself, can only be reproduced by varying the inlet levels of the turbulence scales; while the latter effect can only be simulated through prescribing different inlet radial velocity distributions. Considered first is the response of the predicted flowfield to variations in the turbulence model with V at the inlet set to zero and ϵ held at the reference levels, obtained as described in section II.C.

Figures, 3,4,5, and 6 display the axial variation of the half width, maximum axial, maximum swirl, and centerline velocity, respectively. In Hösel's jet, Rodi's correction is seen to yield fairly close agreement with measurements for $r_{1/2}$, U_m, and W_m while the standard k-ϵ model and, even more so, Launder et al.'s correction (referred to as "LPS" hereafter) underestimate spreading and decay of momentum. None of the three model variants correctly simulate the variation of centerline velocity with Rodi's correction giving the poorest results. The best agreement with Curtet and Darrigol's measurements is, in contrast, achieved with the standard k-ϵ model (except for the far-field spread for $x/d>5$). Here, Rodi's correction overestimates the effects of swirl while the LPS variant again yields low spread and rate of momentum decay.

To clarify the question as to why the LPS correction produces an effect contrary to that expected, the variation of

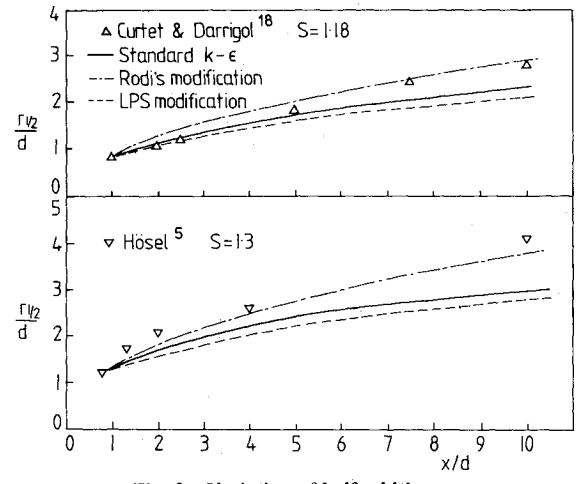

Fig. 3 Variation of half-width $r_{1/2}$.

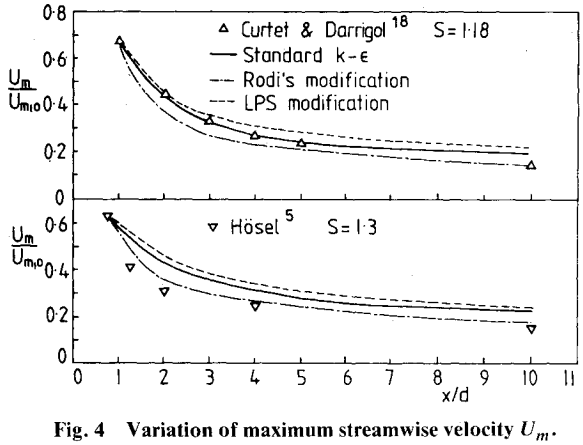

Fig. 4 Variation of maximum streamwise velocity U_m.

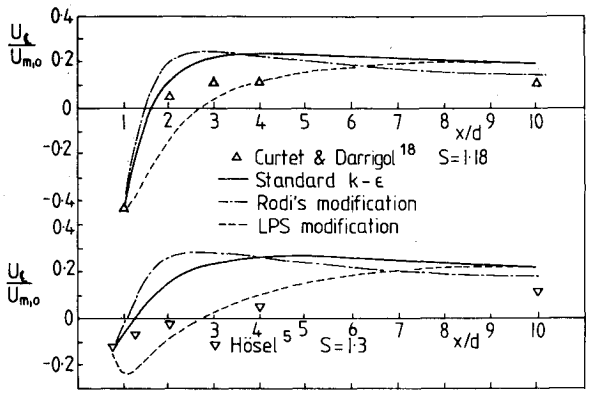

Fig. 5 Variation of centerline velocity U_{ℓ}.

the Richardson number functions f_1 and f_2, as defined by Eqs. (8) and (9), are plotted in Fig. 7 for $x/d=2$, with a cut-off value of zero applied to both functions. It is seen that f_1, representing the LPS correction, produces a turbulence-damping (stabilizing) effect over most of the jet with relatively minor destabilization occurring only in the outer radial zone. This clearly reflects the hypothesis embedded in the correction, according to which destabilization due to streamline curvature relies on a positive radial gradient of centripetal body forces. Such a situation prevails throughout boundary layers developing on rotating bodies—for which the correction was devised—but clearly not in swirling jets. In contrast, Rodi's correction f_2 has a strongly destabilizing effect throughout the jet. Indeed, the effect appears to be excessive even in Hösel's jet, for Fig. 5 shows a rapid erosion of the recirculation zone due to an excessive diffusion of momentum toward the axis of symmetry.

It is of some importance to point out that, while best agreement with experimental data for the two jets is achieved with different turbulence-model variants, the performance of the models is consistent in the two situations. For example, the rates of spread calculated with any one variant are similar, which is not surprising because of the similar inlet conditions used (the spread is slightly larger in Hösel's case because the swirl number and the initial width are larger). This reinforces the conclusion that differences in the initial conditions for either V or/and the turbulence level crucially contribute to the observed differences in the behavior of the jets.

In order to examine the possible extent of this contribution, computations were performed for Hösel's jet with the standard model but with the inlet ϵ and V levels differing from the reference conditions previously used. The inlet ϵ level was varied within the range $0.5\epsilon_r \leq \epsilon \leq 2\epsilon_r$, where ϵ_r is the reference level, while the zero-radial velocity was replaced by the initial V distribution determined from the streamfunction plot, Fig. 2. As seen from Figs. 8-11, halving the reference dissipation (equivalent to doubling the initial shear stress) produces a behavior not dissimilar to that obtained with Rodi's correction. Thus $r_{1/2}$, U_m, and W_m all improve, while agreement in respect of U_{ℓ} deteriorates. Although this deterioration calls into question the realism of substantially deceasing ϵ, the preceding sensitivity test serves to highlight the fact that the initial turbulence level plays a role equal in importance to swirl-related turbulence-model modifications.

A similar conclusion emerges in relation to V, although this test is far less speculative than the former, for V was extracted from U measurements. Thus, Figs. 8-11 show a dramatic improvement in relation to all mean-flow quantities, though some disagreement still persists in the case of U_{ℓ}. It appears, therefore, quite possible that strongly swirling flows can be satisfactorily predicted with the standard version provided close attention is paid to the entire range of initial conditions. Moreover, it seems likely that swirl-related modifications previously used in strongly swirling situations effectively

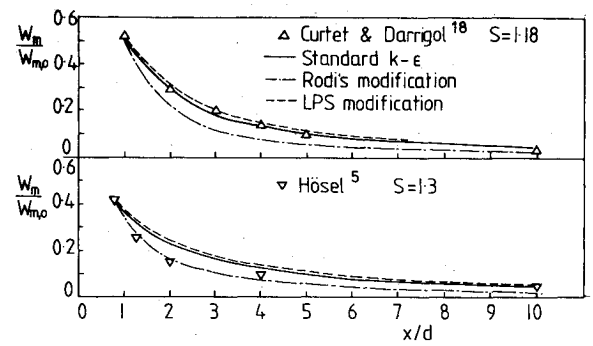

Fig. 6 Variation of maximum swirl velocity W_m.

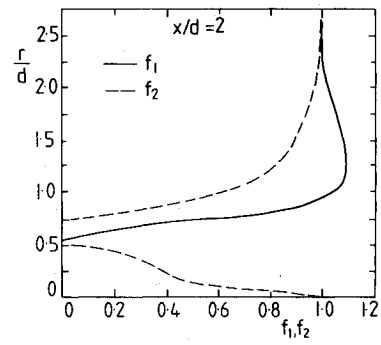

Fig. 7 Radial distribution of correction functions f_1 and f_2 at $x/d=2$ in LPS[11] and Rodi's[8] swirl correction.

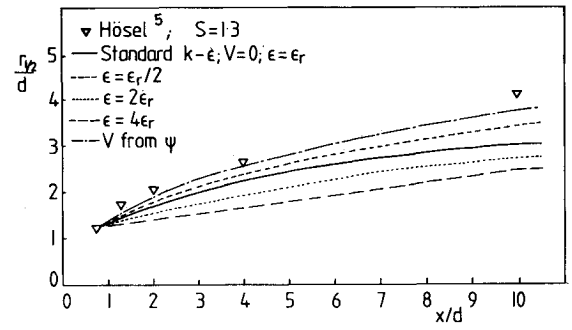

Fig. 8 Variation of half-width $r_{1/2}$ for Hösel's[5] jet; influence of initial ϵ and V.

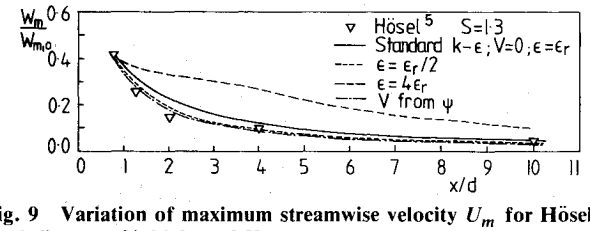

Fig. 9 Variation of maximum streamwise velocity U_m for Hösel's[5] jet; influence of initial ϵ and V.

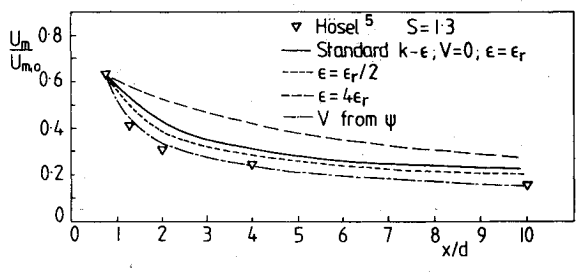

Fig. 10 Variation of maximum swirl velocity W_m for Hösel's[5] jet; influence of initial ϵ and V.

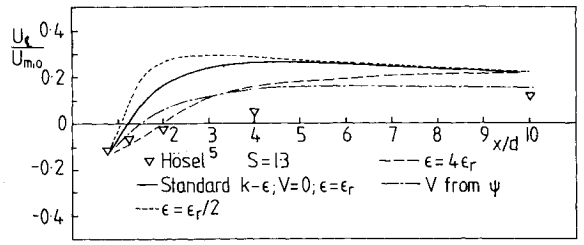

Fig. 11 Variation of centerline velocity U_ℓ for Hösel's[5] jet; influence of initial ϵ and V.

served to hide or compensate for inadequacies in the prescription of boundary conditions. One question which must, unfortunately, remain unanswered here is the reason for the substantial differences in the jet-exit conditions, most probably in the levels of V. An appeal must, therefore, be made to experimenters to always measure and report all exit conditions which can be measured.

IV. Conclusions

The standard k-ϵ model of turbulence and two swirl-specific modifications of it have been applied to simulate two strongly swirling jet situations involving recirculation. The two jets had similar swirl numbers and exit velocity profiles but exhibited quite different spreading behavior, indicating a strong influence of the initial conditions at the nozzle exit. The sensitivity of the calculations to the initial conditions for the quantities V and ϵ, which are known with least certainty from experiments, was examined and found to be fairly strong. This sensitivity makes the assessment of turbulence-model performance a difficult task since disagreement between predicted results may not so much be due to turbulence-model faults as due to the use of inappropriate initial conditions.

A reference initial ϵ distribution was estimated which yields the correct shear-stress level and should, therefore, be not too far from the truth. When this distribution and the specification of zero radial velocity was used in the calculations with the standard k-ϵ model, the jet of Curtet and Darrigol was fairly well predicted; only the spreading was somewhat underpredicted for $x/d \geq 5$. On the other hand, the spreading of Hösel's jet was seriously underpredicted.

A sufficiently different behavior could only be obtained through the use of different initial conditions. Hence, when the unrealistic assumption of zero radial velocity V in Hösel's case was replaced by an initial V distribution determined from the U measurements, fairly good agreement with Hösel's experiments results and the observed difference between the two jets is recovered. As was explained earlier, the asssumption of zero initial V velocity is much more realistic in Curtet and Darrigol's experimental situation.

Rodi's swirl correction was found to increase the effect of swirl on the jet, but with the initial conditions that appear most realistic this effect was excessive, at least in the initial strongly swirling region. The LPS correction reduces the effect of swirl, which is clearly in the wrong direction. This behavior is obvious from the Richardson number definition used in this correction and the Richardson number distribution in swirling jets. The correction is, therefore, inadequate for swirling jets. It appears that the standard k-ϵ model performs best for strongly swirling jets and produces overall fairly good agreement with experiments, while in weakly swirling jets it was found to underpredict the influence of swirl so that corrections are necessary.

Acknowledgments

The work reported here was sponsored by the Deutsche Forschungsgemeinschaft via the Sonderforschungsbereich 80. The calculations were carried out on the UNIVAC 1108 computer of the University of Karlsruhe.

References

[1] Lilley, D. G., "Swirl Flows in Combustion: A Review," *AIAA Journal*, Vol. 15, 1977, pp. 1063-1078.

[2] Morse, A. P., "Flow with Swirl," review submitted to 1980 AFOSR-HTTM-Stanford Conference on Complex Turbulent Flows, 1980.

[3] Smith, J. L., "An Experimental Study of the Vortex in the Cyclone Separator," ASME, *Journal of Basic Engineering*, Vol. 84, 1962, pp. 602-608.

[4] Holman, J. P. and Moore, G. D., "An Experimental Study of Vortex Chamber Flow," ASME, *Journal of Basic Engineering*, Vol. 83, 1961, pp. 632-636.

[5] Hösel, W., "Drallstrahluntersuchungen mit einem weiterentwickelten, Laser-Doppler-Messverfahren," Dr.-Ing. Dissertation, University of Karlsruhe, 1978.

[6] Launder, B. E. and Morse, A., "Numerical Prediction of Axisymmetric Free Shear Flows with a Second-Order Reynolds-Stress Closure," *Turbulent Shear Flows I*, Springer Verlag, Heidelberg, 1979.

[7] Bradshaw, P., "Effects of Streamline Curvature on Turbulent Flow," AGARDograph No. 169, 1973.

[8] Rodi, W., "Influence of Buoyancy and Rotation on Equations for the Turbulent Length Scale," *Proceedings of the 2nd Symposium on Turbulent Shear Flows*, London, Imperial College, 1979, pp. 10.37-10.42.

[9] Leschziner, M. A., "Practical Evaluation of Three Finite-Difference Schemes for the Computation of Steady State Recirculating Flows," *Computer Methods in Applied Mechanical Engineering*, Vol. 23, 1980, pp. 293-312.

[10] Lilley, D. G., "Prediction of Inert Turbulent Swirl Flows," *AIAA Journal*, Vol. 11, 1973, pp. 955-960.

[11] Launder, B. E., Priddin, C. H., and Sharma, B. I., "The Calculation of Turbulent Boundary Layers on Spinning and Curved Surfaces," ASME, *Journal of Fluids Engineering*, 1977, pp. 231-239.

[12] Al-Mohammed, H. H. A., "Flow in Turbulent Coaxial Free Jets with and without Recirculation," Ph.D. Thesis, University of London, 1978.

[13] Boysan, F. and Swithenbank, J., "Numerical Prediction of Confined Vortex Flows, *Proceedings of Numerical Methods in Laminar and Turbulent Flow*, Venice, 1981; also Dept. of Chemical Engineering, University of Sheffield, England, Rept. HIC 370, 1981.

[14] Lilley, D. G., "Primitive Pressure-Velocity Code for the Computation of Strongly Swirling Flows," *AIAA Journal*, Vol. 14, 1976, pp. 749-756.

[15] Boysan, F., Ayers, W. H., Swithebank, J., and Pan, Z., "Three-Dimensional Model of Spray Combustion in Gas-Turbine Combustors," *Journal of Energy*, Vol. 6, 1981, pp. 368-375.

[16] Kubo, I. and Gouldin, F. C., "Numerical Calculations of Turbulent Swirling Flow," ASME, *Journal of Fluids Engineering*, Vol. 97, 1975, pp. 310-315.

[17] Khalil, E. E., Spalding, D. B., and Whitelaw, J. H., "The Calculation of Local Flow Properties in Two-Dimensional Furnaces," *International Journal of Heat and Mass Transfer*, Vol. 18, 1975, pp. 775-791.

[18] Curtet, R. M. and Darrigol, M., "Aerothermique d'un jet libre tournant turbulent," prepared for 6th International Heat Transfer Conference, Toronto, 1978.

[19] Launder, B. E. and Spalding, D. B., "The Numerical Computation of Turbulent Flow," *Computer Methods in Applied Mechanics and Engineering*, Vol. 3, 1974, pp. 269-289.

[20] Sharma, B. I., "The Behavior of Swirling Turbulent Boundary Layers Near Walls," Ph.D. Thesis, University of London, 1975.

[21] Gosman, A. D. and Pun, W. M., Lecture notes for course entitled Calculation of Recirculating Flows, Imperial College, London, Dept. of Mechanical Engineering, HTS/74/2, 1974.

[22] Gosman, A. D., Koosinlin, M. L., Lockwood, F. C., and Spalding, D. B., "Transfer of Heat in Rotating Systems," ASME Paper 76, GT-25, 1976.